MODULAR FRACTAL MEASURES

LINAS VEPSTAS <LINAS@LINAS.ORG>

ABSTRACT. A notable example of a discontinuous-everywhere function that is not traditionally integrable, yet, when properly defined, can be integrated, is derivative of the Minkowski Question Mark function. Some subject matter overlaps that of [6]. This paper includes numerical results for the Fourier transform of the measure, its Mellin transform, and Poisson kernel.

This document is a research diary noting various results, and is haphazardly structured.

This note is a part of a set of papers that explore the relationship between the real numbers, the Cantor set, the dyadic monoid (a sub-monoid of the modular group $SL(2,\mathbb{Z})$), and fractals.

1. INTRO

THIS IS A CLIP-BOOK or DIARY of PARTIALLY-EXPLORED RESULTS. The intro hasn't been written yet, but if it was, it would work like this:

2. DISTRIBUTION OF THE RATIONAL NUMBERS IN THE FAREY TREE

One way to enumerate all of the rationals is by placing them on the Farey tree (or the Stern-Brocot tree). It can be shown that the Farey tree enumerates all of the rationals in the unit interval exactly once [2]. However, the distribution of the rationals on the Farey tree is highly non-uniform, if the tree is walked breadth-first. The figure 2.1 shows that distribution. This distribution is highly non-uniform, and by fooling with the number of bins in the histogram, it becomes clear that the figure is highly discontinuous. As the number of bins is increased, it becomes clear that the distribution has a peculiar structure: it always has a humped form, even though the individual spikes vary strongly according to the number of bins.

The shape is suggestive, and the numerical evidence makes it clear that it is somehow the "derivative" of the Minkowski question mark function $?'(x) = d?(x)/dx$. Performing a simple numeric integral of the above, and comparing it to the exact expression shows a perfect match, as witnessed in the figure 2.2.

A proof of the the equivalence of the distribution of the Farey numbers and the derivative of the Question Mark is given in [7].

The derivative of the Minkowski question mark function cannot be defined using the classical analytic techniques. More precisely, classical analytic tools applied to the "natural" topology of open sets on the real number line are insufficient to construct and describe the shape of this curve. This motivates the study of alternative topologies for the real number line, which constitutes one of the research programs of this paper.

When one does attempt to use classical techniques applied to the classical topology, the result is a number of preposterous-sounding statements, a sampling of which are given

Date: 12 October 2004 (updated 2 November 2008).

FIGURE 2.1. Distribution of Farey Fractions

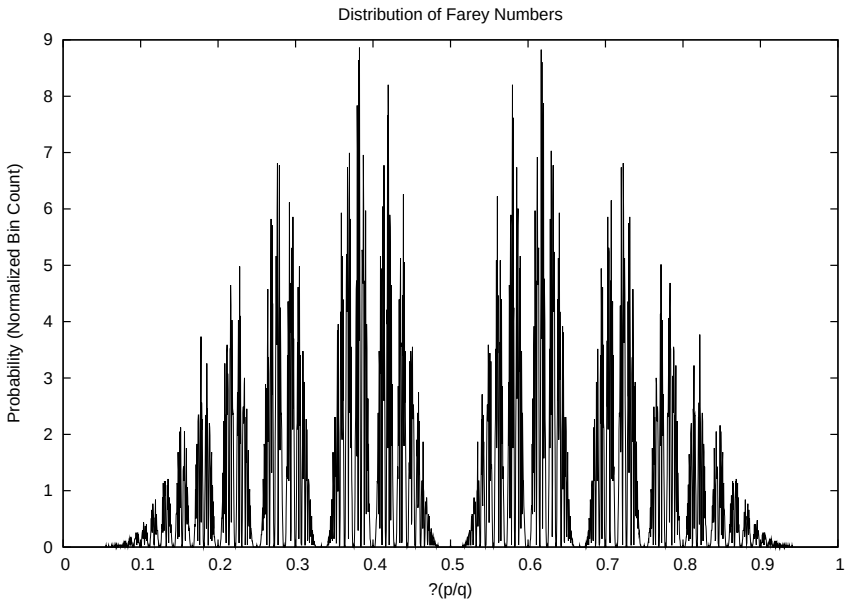

This figure shows a histogram of the first M=65536 Farey fractions according to their location on the unit interval. To create this figure, the unit interval is divided up into N=600 bins, and the bin count c_n for each bin n is incremented whenever a fraction p/q falls within the bin: $(n-1)/N \leq p/q < n/N$. At the end of binning, the count is normalized by multiplying each bin count c_n by N/M. The normalization ensures that the histogram is of measure one on the unit interval: that $\sum_{n=0}^{N} c_n = 1$. In a certain sense, the "shape" of this histogram is independent of the number of bins and number of fractions counted, although on a highly detailed level, the graph clearly varies with the number of bins N. In a proper formal treatment, we would need to show that the limit $\lim_{M\to\infty} c_n$ exists and is finite, for all n and N.

below. The question mark is highly singular. It is infinitely differentiable at every rational, and all derivatives vanish at every rational; yet the mapping is strictly monotonically increasing. Just examining the graph visually suggests that the derivatives must be non-zero "somewhere", although how to define how to value these derivatives is utterly unclear. Naively, they seem to be "infinite" at every irrational; but this fails to explain how to integrate.

Clearly, the classical approach is sorely lacking and inapplicable; something different is needed. Two possibilities arise: throw away traditional ideas of integration and differentiation, and replace them with something new, something suitable for fractals, or keep these tools, but throw away the "natural" topology on the real number line. The latter approach seems to be far more promising. There are several possible alternative topologies. Most immediately obvious is the topology of the Cantor set, which is readily mapped to the real

FIGURE 2.2. Sum of Farey Histogram

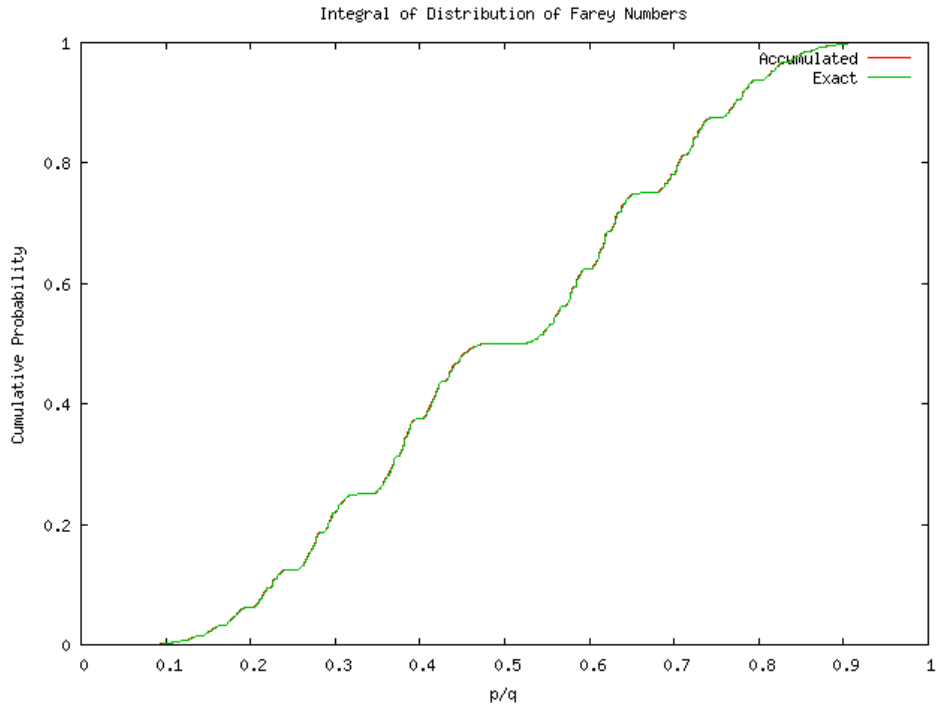

This figure shows the sum of the bin counts of the Farey fractions, together with a graph of the Minkowski question mark function. The two graphs can hardly be told apart.

number line. Less obvious, but more appropriate, is the topology of "cylinder sets" that is the natural topology for studying shifts, symbolic dynamics, and one-dimensional lattice models. A certain limiting case of the Cantor set topology coincides with the language of cylinder sets; this appears to be adequate for constructing measures which can capture the general structure of this distribution.

The figure 2.3 shows what could be called the Jacobian $(?' \circ ?^{-1})(x)$ of the question mark function. This figure simple relabels the x-axis by passing it through $?(x)$. This function appears to vanish only at the dyadics. Note the superficial resemblance of the profile to the Takagi curve. By visually comparing this function and the Takagi curve (also called the *blancmange curve*), one can intuitively sense that there must be a more formal relation between the two, as if the values of the one function could somehow be exponentiated to give the other. The trick is to write down this relation.

This is really a very curious circumstance. The above graphs show only the distribution of a finite number of points (they were, after all, computer generated). A finite set of points on the real number line is zero; yet we are using it to induce a measure that can be used for integration. How is this? The statistical properties of a finite sampling provide us with information about the limit. Its as if we were working with an anti-Cantor-set construction: we start with a dust, and average over intervals to discover analytic properties.

The remainder of this paper proceeds by first examining the Fourier transform of the quantity $(?' \circ ?^{-1})(x)$, followed by the presentation of a class of fractal curves which appear to capture the structure of $(?' \circ ?^{-1})(x)$. This is followed by a discussion of how these

FIGURE 2.3. Jacobian

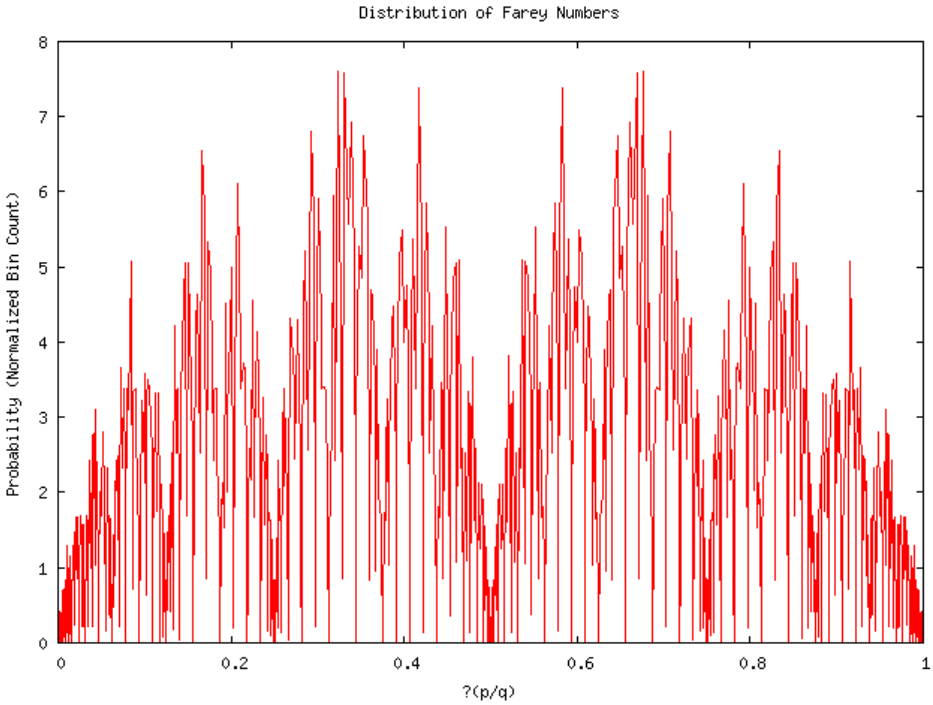

This figure shows the same Farey fraction distribution as in a previous figure, except that the x-axis is relabeled by passing it through the Minkowski question mark. In a certain sense, this can be taken to be the Jacobian $(?' \circ ?^{-1})(x)$ of the question mark.

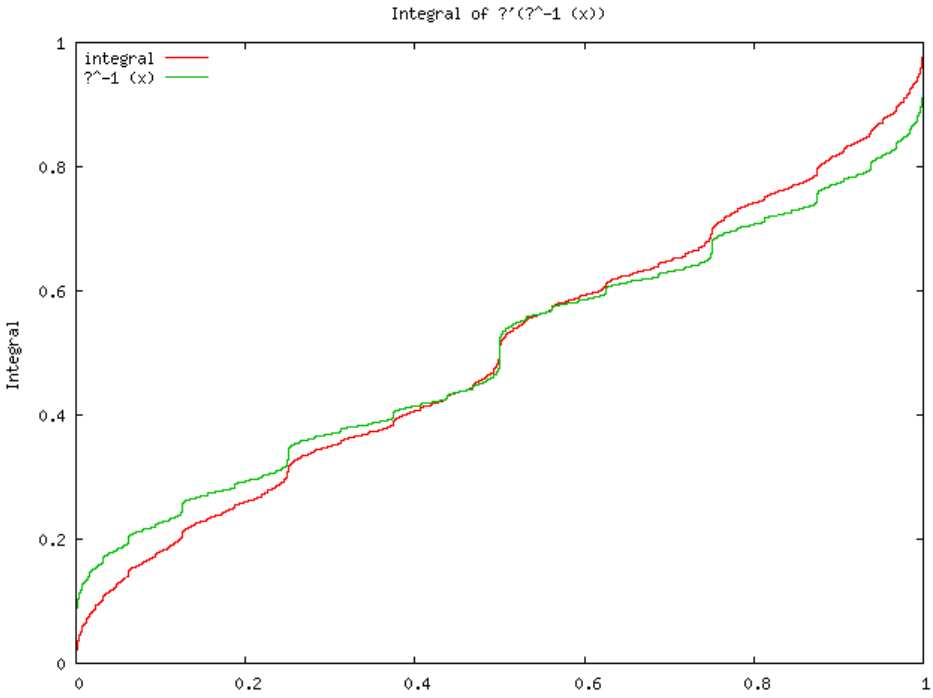

This figures shows the integral $\int_0^x (?' \circ ?^{-1})(y)\,dy$, and, by comparison, the value of $?^{-1}(x)$ which it resembles.

FIGURE 2.4. Takagi Curve

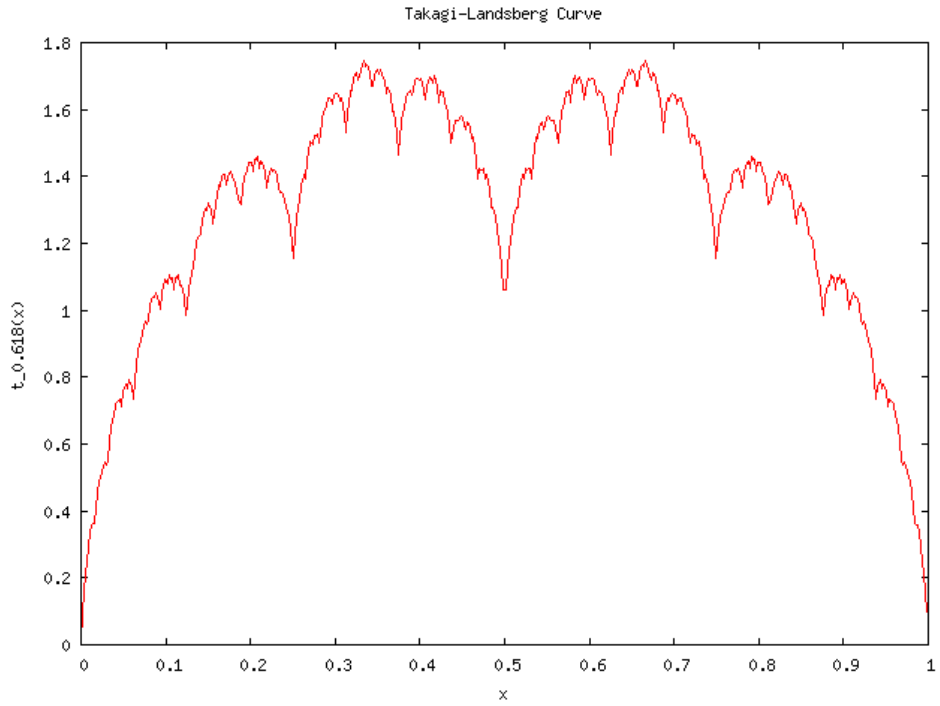

A graph of the Takagi-Landsberg curve $t_w(x)$ as a function of x for a fixed value of $w = 0.618$. Note the curious visual resemblance to the Jacobian of the Question Mark function. The Takagi curve, explored in [5], is given by

$$t_w(x) = \sum_{k=0}^{\infty} w^k \tau\left(2^k x\right) \tag{2.1}$$

where $\tau(x)$ is the triangle function:

$$\tau(x) = \begin{cases} 2(x - \lfloor x \rfloor) & \text{for} \quad 0 \le x - \lfloor x \rfloor < 1/2 \\ 2 - 2(x - \lfloor x \rfloor) & \text{for} \quad 1 > x - \lfloor x \rfloor \ge 1/2 \end{cases} \tag{2.2}$$

The fractal self-symilarity of the Takagi curve is given by a three-dimensional representation of a certain monoid, the "dyadic monoid".

curves can be viewed either as a measure on a Cantor set, or, equivalently, as statistical lattice model.

2.1. **Notes.** Some slightly formal but not very fruitful remarks follow. To prove that the measure vanishes on rationals, one must show two things: first, that the measure vanishes near 0 (or 1), in that the the bin count for bin c_0 (and c_1 and a few neighbors) is always bounded above by $N^{-\alpha}$ for some $\alpha > 1$. In fact, α is probably quite large, and the bound can be made very strong. Next, one needs to show a modular group symmetry for the histogram: thus for example, that $c_{pN/q}$ obeys a similar bound, but de-rated by a factor given by the modular group element that carries $0/1$ to p/q.

FIGURE 3.1. Fourier of Jacobian

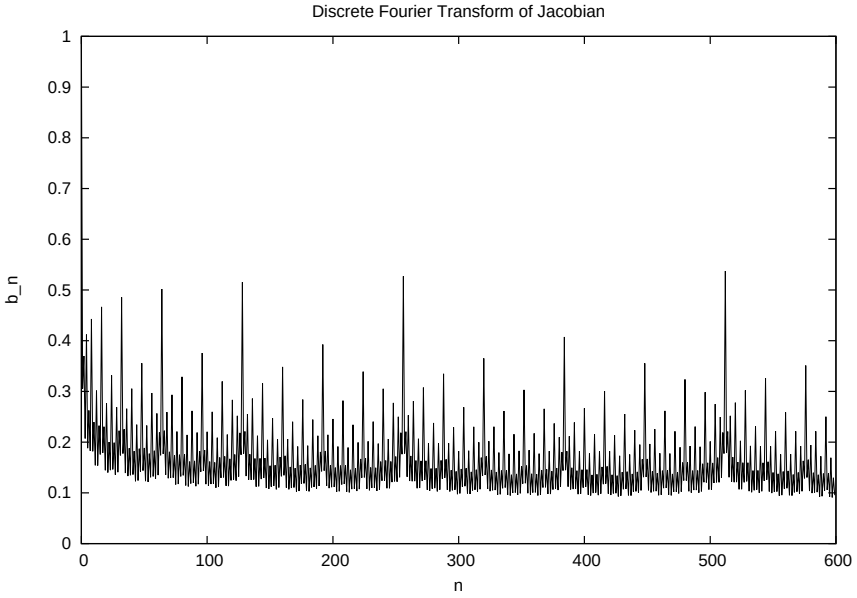

This figure shows the values of the discrete Fourier transform coefficients

$$b_n = \int_0^1 \exp(2\pi i n ?(u))\, du$$

as a function of n. These were computed by numerical integration, by dividing the unit interval into 60,000 uniform-width bins. The principle peaks occur at powers of 2, that is, at 16,32,64,128,256, and so on. Lesser peaks clearly subdivide the intervals between these peaks.

3. JACOBIAN AND ITS FOURIER TRANSFORM

Consider the integral

$$b_n = \int_0^1 \exp(2\pi i n x) \frac{dx}{?'(?^{-1}(x))}$$

Because the denominator is discontinuous everywhere, the above is not well-defined without additional work. Noting the denominator is in the form of a Jacobian, naively performing the change of variable $u = ?^{-1}(x)$ leads to

$$b_n = \int_0^1 \exp(2\pi i n ?(u))\, du \tag{3.1}$$

This last expression is easily evaluated by numerical means. By symmetry of the question-mark function, the coefficients are purely real. A graph of these coefficients are shown in figure 3.1. A fractal self-similarity is clearly evident.

Numerical access to these coefficients begs a question: what would the inverse transform look like? Formally, the inverse is given by

$$\begin{aligned}\frac{1}{?'\left(?^{-1}(x)\right)} &= \sum_{n=-\infty}^{\infty} b_n e^{-2\pi i n x} \\ &= b_0 + 2\sum_{n=1}^{\infty} b_n \cos(2\pi n x)\end{aligned}$$

This function is, again, easily accessibly by numerical means; it is shown in figure 3.2. The structure shown in the figure is highly suggestive: it appears to be an arrangement of Dirac delta functions of varying strengths, located at the dyadic rationals. The structure is not entirely straight-forward, but a hypothesis for this distribution is presented in the next section.

By differentiating the identity $x = ?\left(?^{-1}(x)\right)$ one obtains the simple identity

$$\left(?^{-1}(x)\right)' = \frac{1}{?'\left(?^{-1}(x)\right)} \tag{3.2}$$

and so the figure 3.2 can be thought of as illustrating the derivative of $?^{-1}(x)$. The figure confirms the intuition of what this derivative should look like: the derivative becomes infinite (Dirac delta-function spikes) at the dyadic rationals. This figure could be prepared directly, without the intervening Fourier transform: one could simply bin-count uniformly-generated values of x, passing them through $?^{-1}(x)$ and thence into bins. Numerically, bin-counting in this direct fashion is both easier and less prone to noise from rounding and cutoff effects. The result of direct counting confirms the accuracy of 3.2, as well as suggesting another curious detail. On close examination of this figure, it appears that there are small areas of non-vanishing support at the dyadics. These are largest, and thus most clearly visible, under the peaks at 0 and 1, and again, but smaller, at 1/2. Whether these are numerical artifacts, or are real condensation points is hard to say. These are magnified and shown in figure 3.3. The overt structure of figure 3.2 suggests that this function consists solely of Dirac delta functions located at the dyadic rationals. The magnified figure 3.3 suggests that the function $d?^{-1}(x)/dx$ might take on non-zero values at the other rationals, or even at the irrationals – this is what is meant by "real condensation points". Without a formal, "analytic" expression for $d?^{-1}(x)/dx$, it is impossible to decide whether this feature is "real" or an artifact.

The idea that these might be real condensation points is gugested by the fact that in each sequence of delta functions, the magnitude of the delta function does not decrease to zero at the limiting point of the sequence, but remains non-zero. Each dyadic rational is the limit point of many such sequences.

Proceeding in a similar manner, one can obtain

$$c_n = \int_0^1 \exp(2\pi i n x)\, ?'\left(?^{-1}(x)\right)\, dx$$

by performing a change of variable:

$$c_n = \int_0^1 \exp(2\pi i n ?(u))\, \left[?'(u)\right]^2\, du$$

and then evaluating the above by means of bin-counting, the point being that it is straightforward to bin-count $?'(u)$, whereas there are grave numerical difficulties with numerically arranging bin-counts of $?'\left(?^{-1}(x)\right)$. The results of such counting are shown in figure 3.4.

FIGURE 3.2. The Jacobian by Inverse Discrete Transform

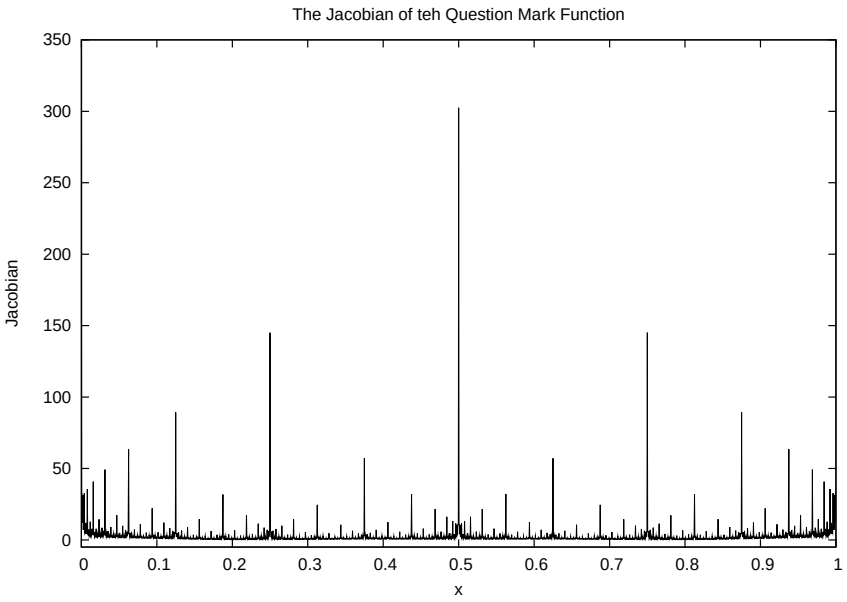

The above figure shows the value of the Jacobian, computed numerically, by means of the equation

$$\frac{1}{?'\left(?^{-1}(x)\right)} = b_0 + 2\sum_{n=1}^{\infty} b_n \cos(2\pi n x)$$

Clearly, one has $b_0 = 1$,and so the figure actually shows

$$\frac{1}{?'\left(?^{-1}(x)\right)} - 1$$

in order to emphasize that the distribution is about zero. The principle peaks are at inverse powers of two, namely, at

$$\frac{1}{2}, \frac{1}{4}, \frac{1}{8}, \frac{1}{16}, \cdots$$

Although the principle peaks decrease in size, they do not do so linearly. Nor is the size distribution regular, in the sense that the peaks at 3/8 and 5/8 are significantly smaller than those at 1/8 and 7/8. A hypothesis for the actual size distribution is discussed in the text.

By contrast, the Fourier coefficients of just plain $?'(x)$ do not exhibit any such regular pattern, and instead give the general appearance of noise. These are shown in figure 3.5. Similar remarks apply to the case of $1/?'(x)$. The conclusion to be drawn here is that by failing to employ the inverse $?^{-1}(x)$ together with the derivative, the structure if randomized out during the averaging process imposed by the Fourier transform. Put another way, by failing to employ $?^{-1}(x)$, one is effectively taking the averages "in the wrong space";

FIGURE 3.3. Closeup of Derivative

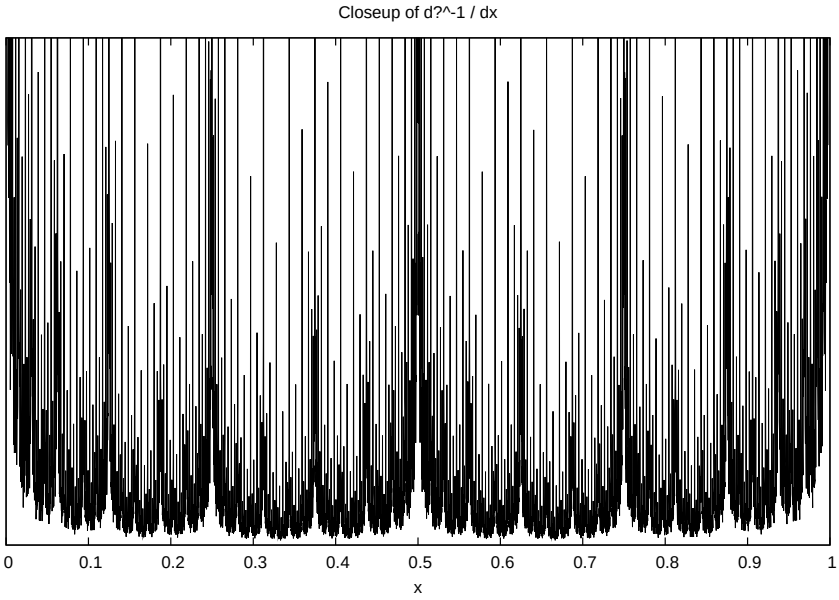

This figure provides a closup view of the graph near the origin, of the function shown in figure 3.2. However, rather than obtaining this figure by Fourier-transform, it was instead obtained by direct bin-counting. That is, a sequence of 256 million pseudo-random numbers were generated, lying between 0 and 1. Then $?(x)$ was computed for these numbers, and the result was added into one of 4097 bins. The bin counts ae then graphed directly. Note that the graph fails to touch down at the x-axis, but rather has rounded corners.

by using the $?^{-1}(x)$, one pulls the map back into the space over which the distribution is taking place. This is why there is a very clean structure in figures 3.1 and 3.4, while the structure of 3.5 is essentially that of noise.

Unfortunately, the structure seen in figures 3.1 and 3.4, while being very suggestive, does not yet allow any simple guess as to what that structure is, exactly. In particular, charting the heights of the peaks shows that the heights are not linear or geometric or logarithmic in size. In particular, as a sequence of peaks approaches a cluster point, the height of the peaks do not appear to decrease to zero, but rather to a finite value; the nature of that value is unclear.

4. MELLIN TRANSFORM

Of some curiosity is the analytic structure of the Mellin transform of the Minkowski derivative and measure. Figure 4 illustrates the quantity

$$\int_0^1 x^s ?'(x)\, dx$$

FIGURE 3.4. DFT of Inverse Jacobian

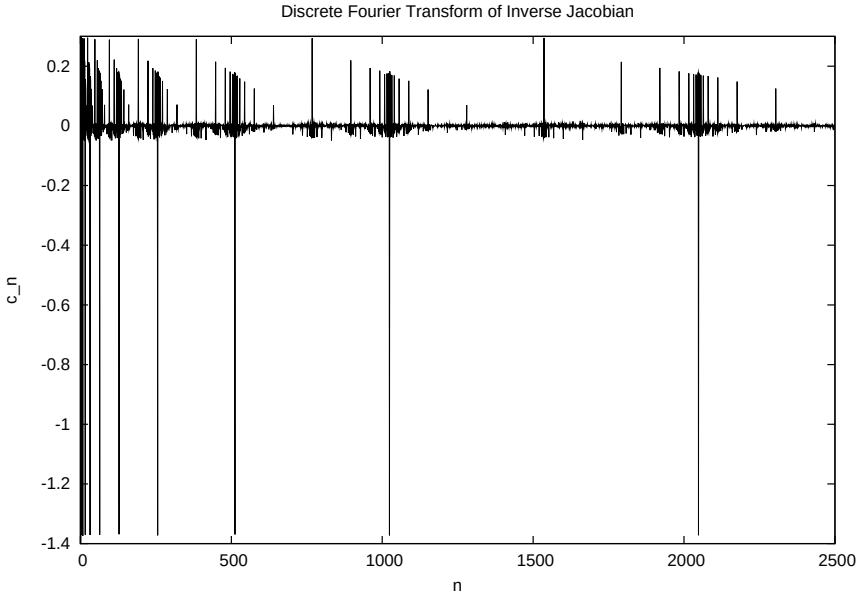

This figure shows the coefficients

$$c_n = \int_0^1 \exp\left(2\pi i n ?\left(u\right)\right) \left[?'\left(u\right)\right]^2 du$$

for the range $1 \leq n \leq 2500$ obtained by bin-counting the first 32 million Farey fractions into 4.6 million bins. The "noise" in the figure is best eliminated by moving to an ever-greater number of bins. Visible are sharp spikes, of equal height, that occur at $n = 2^m$ for integer m. Also clearly visible is a sawtooth of spikes that "chirp" as they approach the primary spikes. There also appears to be additional structure, although it is difficult of make out visually at this scale.

for general complex-valued s, whil 4 shows

$$\int_0^1 x^s ?'\left(?^{-1}\left(x\right)\right) dx$$

It is of some curiosity to note that the analytic structure exhibits no obvious crazy fractal patern; it seems to be well-mannered overall, and appears to be "just another holomorphic function". This would seem to indicate that the inverse Mellin transform of "plain-old" holomorphic functions can be quite astonishing, in general.

5. POISSON KERNEL

The Poisson kernel commonly occurs in the study of Hardy spaces, and occurs there in several contexts. The most notable is in a theorem of F. Reisz, the decomposition of

FIGURE 3.5. DFT of the Derivative

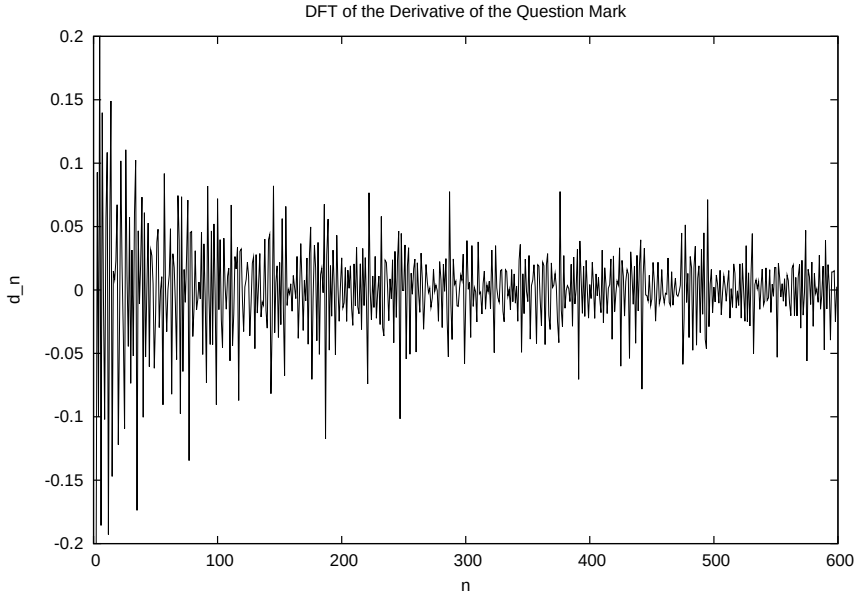

This figure shows the Fourier coefficients given by

$$d_n = \int_0^1 \exp(2\pi i n x)\, ?'(x)\, dx$$

obtained for $0 \le n \le 600$ by bin-counting the first 16 million Farey fractions into 1.6 million bins. Unlike the previous figures, this shows no obvious fractal or self-similar structure.

bounded holomorphic functions into inner, outer, and singular functions. Given the singular nature of the Question Mark, the question of its extension to the complex plane is interesting.

Given a singular measure $d\mu$, the Possion kernel yeilds a holomorphic extension:

$$g(z) = \int_0^1 \frac{e^{i2\pi t} - z}{e^{i2\pi t} + z} d\mu(t)$$

Here, t is understood to be real, so that $d\mu(t)$ is a measure on the unit interval; whereas z is any value on the complex plane (although it is typically taken to be inside the unit disk.

For the case of the Question Mark, by taking

$$d\mu(t) = \left(?' \circ ?^{-1}\right)(t)\, dt$$

a numerical exploration suggests that

$$g(z) = \begin{cases} +1 & \text{for } |z| < 1 \\ -1 & \text{for } |z| > 1 \end{cases}$$

FIGURE 4.1. Mellin transform of the Minkowski derivative

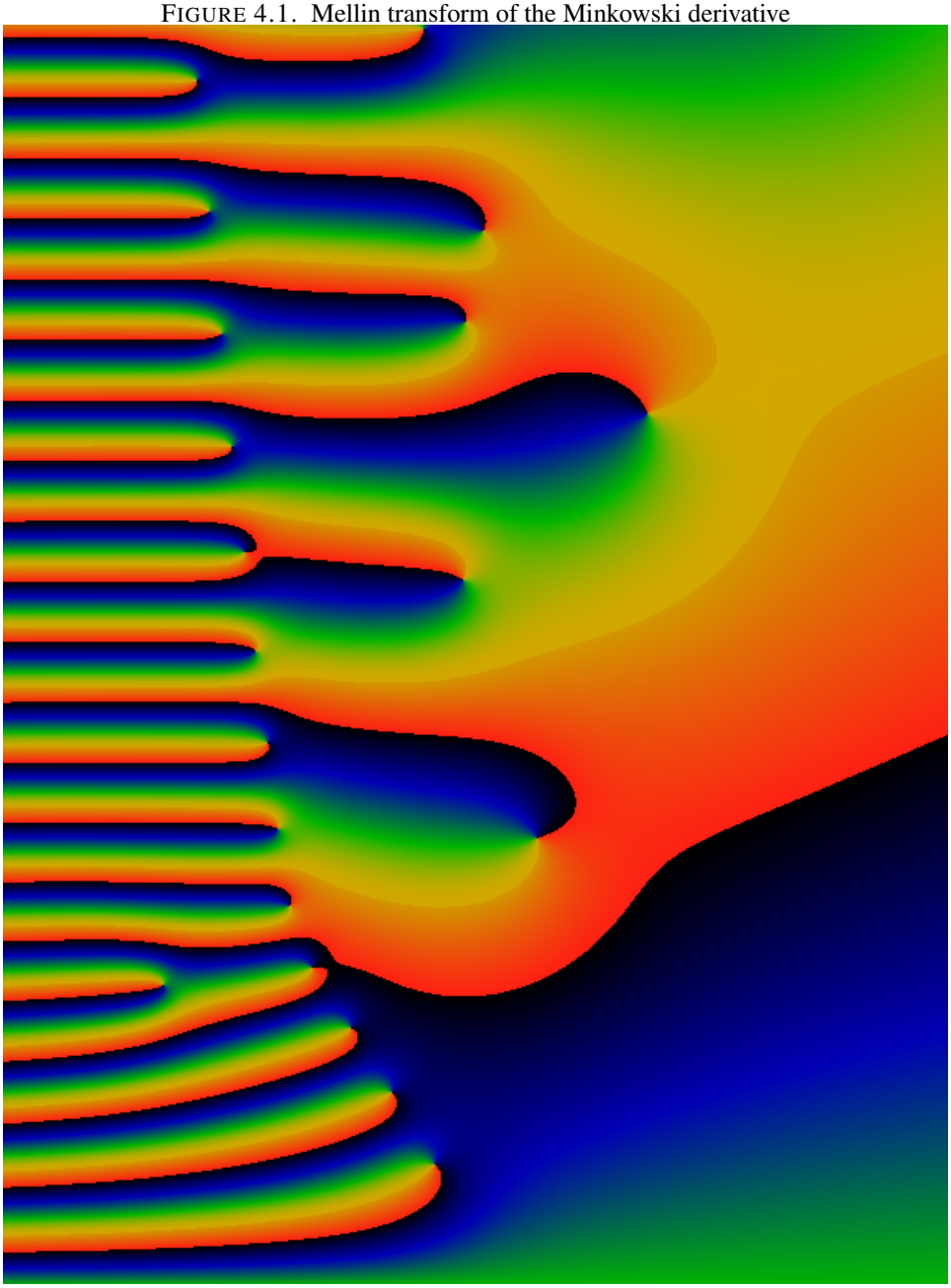

This figure illustrates the Mellin transform for the Minkowski derivative. That is, it shows the phase of the integral

$$\int_0^1 x^s ?'(x)\,dx$$

for general, complex-valued s. Specifically, it shows the region $-15 \leq \Re s \leq 15$ and $0 \leq \Im s \leq 40$. The phase runs from 0 to 2π, of course, and the coloration is such that black represents a phase of 0, red a phase of 2π, and the other colors interpolating in between, with yellow being approximately a phase of π. Simple poles are clearly seen at the terminus of the "fingers", (where the phase wraps around completely).

FIGURE 4.2. Mellin Measure

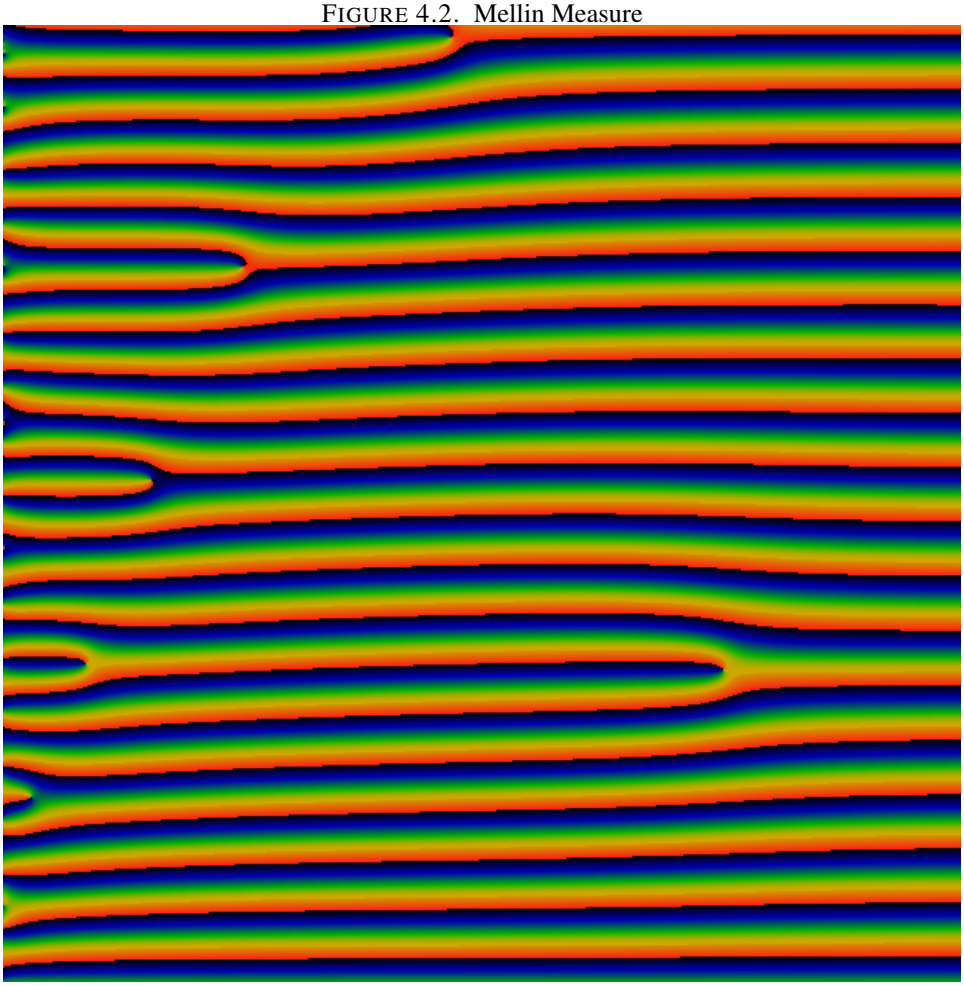

This figure illustrates the Mellin transform for the Minkowski measure. That is, it shows the phase of the integral

$$\int_0^1 x^s ?' \left(?^{-1}(x)\right) dx$$

for general, complex-valued s. Specifically, it shows the region $0 \leq \Re s \leq 160$ and $0 \leq \Im s \leq 160$. The coloration is the same as in figure 4. As before, simple poles are clearly seen at the terminus of the "fingers", (where the phase wraps around completely).

However, as a numerical result, this is very weak. Almost any non-negative distribution on the unit circle will evaluate numerically to a very similar result.

6. DELTA-FUNCTION DISTRIBUTIONS

The distribution for equation 3.2 shown in figure 3.2 is suggestive and open to hypothesizing. This section develops a family of distributions exhibiting the same general

properties as this figure; they are composed of sequences of Dirac delta functions. It is hyypothesized that one member of this family is exactly the desired distribution.

Consider first the "main sequence" of delta fuctions, which seem to be of the form

$$\delta(x-1)+\frac{1}{2}\delta\left(x-\frac{1}{2}\right)+\frac{1}{4}\delta\left(x-\frac{1}{4}\right)+\ldots$$

A close examination of the numerical data shows that the main sequence of peaks is not this simple; in particular, it does not have this geometric progression of sizes. However, the above sequence also doesn't have the full fractal self-similarity; perhaps linear combinations of the above can lead to the desired shape. Towards this end, define a "main sequence" funtion as

$$h_w(x)=\sum_{n=0}^{\infty} w^n \delta\left(1-\frac{1}{2^n}\right)$$

Here, w is to be a parameter; its expected that $w<1$. A symmetrized version of this function is

$$j_w(x)=h_w(x)+h_w(1-x)$$

A fully self-similar arrangement of delta functions can then be arranged by the same construction as that of the Takagi function; furthermore, this construction can be proven to have exactly the same set of self-symmetries and self-similarity transformation properties as the question mark itself [5]. The construction proceeds by defining

$$\tilde{j}_w(x)=j_w(x-\lfloor x\rfloor)$$

where $\lfloor x\rfloor$ is the floor of x. The self similar fractal is then given by

$$k_{vw}(x)=\sum_{k=0}^{\infty} v^k \tilde{j}_w\left(2^k x\right)$$

where v is another, independently adjustable parameter. A numerical exploration of this function suggests that the actual distribution might be near to $v=0.42$ and $w=1.0$, that is, the hypothesis is that

$$\frac{d?^{-1}(x)}{dx}\sim k_{0.42,1}(x)$$

The meaning of the value of 0.42 is unclear. A graph of this distribution does hint slightly at the rounding effect shown in figure 3.3, but is not anywhere near as pronounced.

7. A Family of Cantor-set Distributions

The family of delta-function distributions suggests how to construct a notion of thier reciprocal. The reciprocal should be zero where-ever there is a delta function, and have a non-zero measure wherever the delta-function distribution was zero; in this case, at the irrationals. Such a measure can be explicitly constructed; the construction can be laid on solid foundations, as a measure on the Cantor set. Before formalizing, this measure is first built by example.

The function

$$s_w(x)=\begin{cases} w^n & \text{for } \frac{1}{2^{n+2}}<x<\frac{1}{2^{n+1}} \\ 0 & \text{for } x=\frac{1}{2^n} \\ s(1-x) & \text{for } \frac{1}{2}<x \end{cases}$$

has the shape of a stupa-like stepped pyramid, shown below for $w=1/2$:

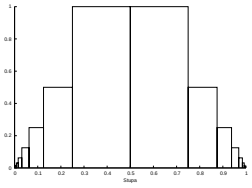

This may be used to construct a Cantor-set measure, by defining

$$\mu_w(x) = \frac{1}{Z}\prod_{k=0}^{\infty} \tilde{s}_w\left(2^k x\right) = \frac{1}{Z}\exp\sum_{k=0}^{\infty} \log \tilde{s}_w\left(2^k x\right) \tag{7.1}$$

where the tilde-version of a function is defined as before,

$$\tilde{s}_w(x) = s_w(x - \lfloor x \rfloor)$$

The normalizing factor Z (which will be revealed to be the *partition function*) serves to normalize the measure, so that

$$1 = \int_0^1 \mu_w(x)\, dx$$

That eqn 7.1 deserves to be called a measure on a Cantor set will be explained in a later section. First, note that the summatation is in the same form as the sumation that is used to define the Takagi or blancmange curve. Taking this as a cue, the measure can be slightly generalized by adding another parameter v:

$$\log \mu_{v,w}(x) = \sum_{k=0}^{\infty} v^k \log \tilde{s}_w\left(2^k x\right) - \log Z \tag{7.2}$$

This family of measures is numerically tractable, and a quick check suggests that the shape depected in figure 2.3 belongs to this family. Numerical exploration suggests a hypothesis, that the correct shape is not far from $v = 0.73$ and $w = 0.78$; that is, one has the approximate numerical identity

$$?'\left(?^{-1}(x)\right) \approx \mu_{0.73,0.78}(x)$$

The true origin of these fractional values for v and w is unclear; in the present case, they were arrived at by numerical means, by exploring the integral

$$Q_{v,w}(x) = \int_0^x \mu_{v,w}(?(y))\, dy$$

so that the actuial numerical approximation is given by

$$?(x) \approx Q_{0.73,0.78}(x) \tag{7.3}$$

The self-similarity transformation properties of Q and μ can be explored by the same techniques as those developed for the Takagi curve, in [5]. This is possible because the construction of eqn 7.2 directly corresponds to that used for the Takagi curve.

8. Cantor Measures

This section takes a brief moment to justify the label of "Cantor set measure" used in the paragraphs above. It proceeds by the definition of the canonical Cantor set, then a class of Cantor sets with non-zero measure, and finally, a class of generalized Cantor sets with arbitrary measures.

The traditional Cantor set is constructed by considering first the closed unit interval, and then removing the open set that is the middle third: by removing the set $(1/3, 2/3)$. One then removes the middle thirds from the remaining two closed intervals, and then

recursively proceeding *ad infinitum*. It was Cantor's achievement to show that the remaining set is uncountable [3]. This procedure can be performed multiplicatively; namely, by considering the function

$$c(x) = \begin{cases} 1 & \text{for } 0 \le x \le \frac{1}{3} \\ 0 & \text{for } \frac{1}{3} < x < \frac{2}{3} \\ 1 & \text{for } \frac{2}{3} \le x \le 1 \end{cases}$$

The indicator function for the Cantor set is then given as

$$\mu_C(x) = \prod_{k=0}^{\infty} \tilde{c}\left(3^k x\right) \tag{8.1}$$

with the tilde defined as before. This indicator function is equal to 1 for any point x belonging to the Cantor set, and zero otherwise. A formal measure, defined in standard measure-theoretic terms, can be defined for this function. In plainer language, it is integrable: one finds that

$$0 = \int_0^1 \mu_C(x)\, dx$$

that is, the measure of the Cantor set is zero. The principal difficulty of constructing the formal measure is the realization that the standard open-interval topology for real interval won't do.

The indicator function above can be generalized in a variety of ways; the most important generalization for the present purposes is to define a measure that is not vanishing on the unit interval. This may be done by considering an indicator function of the form

$$c_w(x) = \begin{cases} 1 & \text{for } 0 \le x \le w \\ 0 & \text{for } w < x < 1-w \\ 1 & \text{for } 1-w \le x \le 1 \end{cases}$$

indicating a pair of closed intervals of width w, which is then recursively compounded by the middle-thirds construction. But geometrically increasing the widths, so as not to get zero measure. – it must get "fat", Etc.

But the above is not the most convenient form for this construction. Sigh. The rest of this section needs to continue the expository review, culminating in the realization that eqn 7.1 really is a proper measure on a Cantor set.

9. INTRO TO REMAINDER

The remainder of this paper should be split off to be its own thing, as it no longer hangs with the above.

Modular forms are analytic functions that are closely related to elliptic functions, and have a particular kind of modular group symmetry. Modular forms are defined on the upper-half plane $\mathbb{H}$ of the complex plane $\mathbb{C}$, that is, for complex numbers $\tau = x + iy$ with $y > 0$ [1]. Here, we are concerned with the limiting behavior of $y \to 0$, which yields highly singular functions defined on the real number line, yet inheriting a modular group symmetry of the form of which they are the limit.

Most fractals presented in the popular literature have a form that suggests that they live on the closure of the hyperbolic plane: that is, they live on the "edge" of that plane. Of course, the hyperbolic metric never allows you to get to that edge, but one can also put an ordinary Euclidean metric on the Poincare disk, or the Poincare upper half plane, and get to that boundary. The problem is, of course, that the topologies that seem to suggest

themselves in these two cases are subtly incompatible, and lead to a variety of confusions. In particular, we argue below that when considering the limiting behavior of of functions at the "edge" of hyperbolic space, the correct topology is a kind of "binary tree topology", similar in form to the Cantor set, but a bit richer. In particular, this topology is finer than the usual topology on the real number line, and this additional fineness allows otherwise dubious expressions to be given precise meaning. It is only when functions on this topology are mapped back onto the real number line that confusions result.

10. A BINARY TREE TOPOLOGY

Consider the "dyadic topology": every rational of the form $p/2^n$ for p odd and integer $n > 0$ is taken to be an open set. All points in between such dyadic rationals are taken to form an open set.

One way to visualize this topology is as a binary tree. At the root of the tree is the point 1/2. At the next level, there is 1/4 and 3/4, and so on. Every such node in the tree is then taken to be an open set. At the leafs of the tree lie the irrationals, and the rationals not of the form $p/2^n$.

The topology differs from that of the canonical Cantor set: in that case, the intermediate nodes are not even considered to be a part of the topology. The leaf nodes are taken to be closed sets, which is how the Cantor set becomes a perfect set.

The point of introducing this binary tree topology is .... Task: construct measures on this topology.

Several remarks are in order. First, in the canonical Cantor set, each leaf was assigned a measure of zero. It should be clear that this choice is arbitrary, and that any measure can be assigned to the endpoints. The cardinality of the endpoints of the binary tree is the cardinality of the continuum, as can be seen by using more or less the same arguments used to discuss the cardinality of the Cantor set. Because of this, it is not unreasonable to believe that one may be able to construct measures that "make sense" in the context of the real number line. In particular, such measures can make well-defined integrals and the like.

Of interest are measures that are functions of, and possibly holomorphic functions, of the dyadic expansion. That is, consider the series $\{b_k : b_k \in \{0,1\}, k \in \mathbb{N}\}$of binary digits given by the dyadic expansion of a real number x:

$$x = \sum_{k=1}^{\infty} \frac{b_k}{2^k} \tag{10.1}$$

This expansion is not unique, because for every dyadic number, there are two inequivalent expansions. For example, $1/2 = 0.1000.. = 0.0111....$ Therefore, we conclude that the dyadic topology is finer than the the usual topology on the real numbers. In particular, the dyadic topology distinguishes all three of these cases: 1/2 is a not in the middle of the tree (the root as it happens here), whereas the two inequivalent expansions belong to two different leafs at the end of the binary tree.

Because this topology is finer than the usual topology on the real number line, one can define functions on this topology that would be ill-defined when considered on the real number line: in particular, the three points above map to just one point on the real numbers. However, it should be painfully clear at this point that this topology is compatible with the discussion the structure of dyadic fractals. It should also be clear that this topology is compatible with discussions of the closure of the upper half-plane when considering the limiting behavior of modular forms, Fuchsian groups, and ergodic processes.

As an example, consider the Takagi curve. When considered on the real-number line, it has a derivative that seems to be defined nowhere. When considered on the binary tree topology, its derivative looks a lot less intimidating: in fact, it is perfectly well-defined on the leaves; the only ambiguity is on the interior nodes of the tree. Furthermore, the interior nodes of the tree are a countable set, whereas the leaves are uncountable.

XXX Discuss "fat cantor set", i.e. a measure which puts all of the measure on the leaves of the tree.

This implies that the derivative of the Takagi curve is in fact defined "almost everywhere", with the exception of only a countable set of points. The goal here is to bootstrap this realization into providing a wholesome topological definition for all fractal measures.

Next, because the topology is that of a binary tree, it should be clear that any binary structure inherits this topology in a natural way. In particular, the Stern-Brocot tree has this topology. In particular, this means that there is a second natural mapping to the real number line, given by the Minkowski Question Mark function. The interior nodes of the tree are the rational numbers (a countable set), and the leaves of the tree are the irrationals (of the cardinality of the continuum). By using the dyadic topology, the derivative of the question mark function becomes a whole lot less intimidating as well: it becomes clear that the derivative is precisely zero on the rationals (the interior nodes of the tree), and non-zero on the leaves. Again, because of the cardinality of the leaves, it becomes clear that this measure can be integrated in a well-founded way. The problem then is no longer "how can the derivative of the question mark be put on a good foundation", rather it becomes "what sort of easy to manipulate, easy to handle expressions for this measure can be found?".

XXXX ToDo: review standard topological notions for the binary tree topology in greater detail, such as separation axioms, bases, metrics, continuity, differentiability. etc. Note that finer topologies typically have fewer continuous, smooth functions than coarse topologies. Since this is finer than the "natural" topology on the reals, who are the losers?

11. Modular Forms

A meromorphic function $f(\tau)$ is said to be a modular form of weight k if it has the modular group symmetry

$$f\left(\frac{a\tau+b}{c\tau+d}\right) = (c\tau+d)^k f(\tau) \tag{11.1}$$

for integers a, b, c and d such that $ad-bc=1$. Here, τ is a complex number, restricted to the upper-half plane: $\Im\tau > 0$. Modular forms can also be expressed as a function of the nome $q = \exp i\pi\tau$. In this form, many have the interesting property of having poles and zeros closely interspersed at the limit of $|q| \to 1$, with poles (or zeros) occurring at rational angles, and the other at irrational angles. A particular example of this is the twenty-fourth root of the modular discriminant, known as the Dedekind eta.

The figure 11.1 shows a particular cross-section through the Dedekind eta. Note the suggestive shape of this curve, and how it crudely resembles the distribution of the Farey fractions. Although it is clear that this curve will not converge to the derivative of the question mark in the limit $|q| \to 1$, it none-the-less is suggestive. Notably, modular forms already have the modular group symmetry, and so already have the symmetry properties of the final curve that we are searching for. This is unlike the histograming approach, where the symmetry is obtained only in the limit. The other remarkable property is that modular forms are infinitely differentiable, and thus posses well-behaved analytic properties, again allowing a kind of study that is ill-afforded by the histograms.

FIGURE 11.1. Dedekind Eta

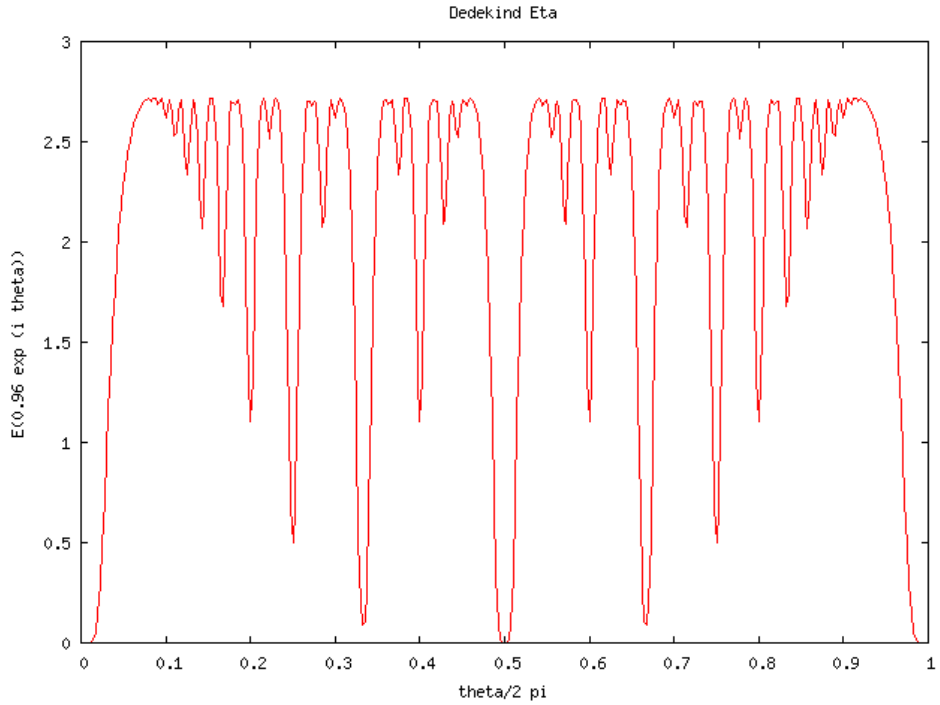

This figure shows a particular slice through the Dedekind eta function $\eta = q^{1/24}\Pi_{n=1}^{\infty}(1-q^{2n})$. This figure graphs $|\eta|$ along a particular curve: we take $q = |q|e^{i\theta}$ and hold $|q| = 0.96$ fixed, while sweeping through values of θ from 0 to 2π. Several features of this figure should be noted. First, this function is continuous and infinitely differentiable for any value of $|q| < 1$. Next, the Dedekind eta has a kind of modular group symmetry: if we write the nome $q = \exp(i\pi\tau)$, then $|\eta((a\tau+b)/(c\tau+d))| = |\sqrt{c\tau+d}\,\eta(\tau)|$ for integers a, b, c, and d such that $ad-bc = 1$. Finally, in the limit of $|q| \to 1$, this function has a zero for all rational angles $\theta = \pi m/n$ where m, n are integers, but otherwise this function diverges for all non-rational angles θ. As such, it has a superficial resemblance to $d?(x)/dx$.

The presumption made here is that the derivative of the Minkowski question mark function will be found to be the limit of some modular form, although which modular form that might be is not clear. The theory of modular forms is deep and broad, and will not be reviewed here. A very synoptic overview can be found in the article on elliptic functions in Wikipedia. There are many deep expositions on the topic [1] [4].

12. CONCLUSION

In conclusion, we conclude ??? We conclude that the ourier transform is very nearly tractable. The sruprising result for the Poisson kernel is begging to be studied in greater detail.

FIGURE 11.2. Sigma angular cross section

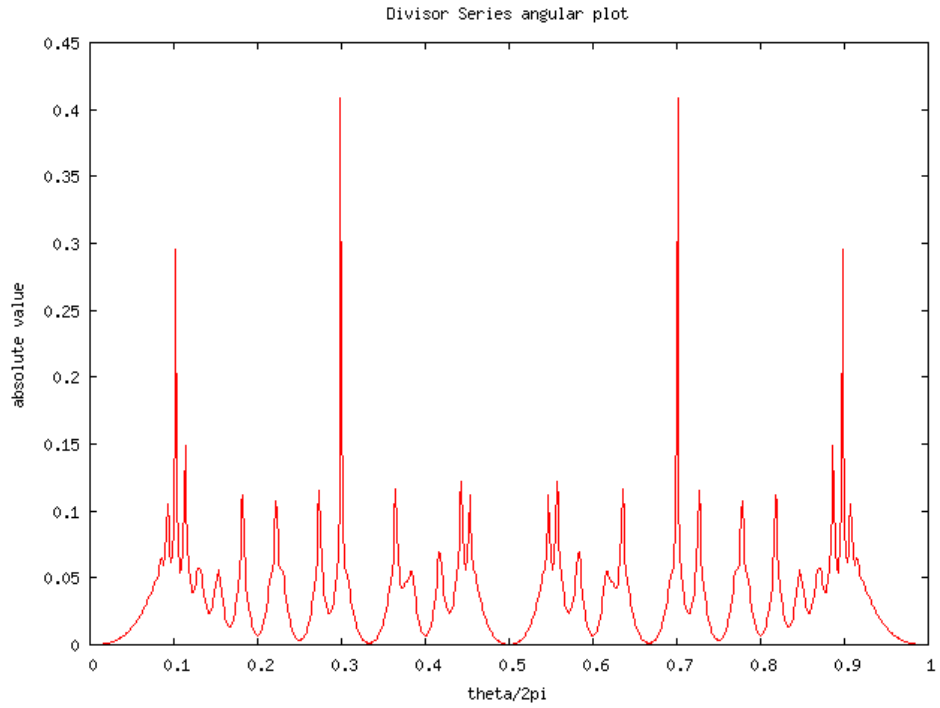

This figure shows an angular cross section of a series build from the number-theoretic divisor function. Specifically, it is a graph of

$$\left| \sum_{n=1}^{\infty} \sigma_2(n) r^n e^{in\theta} \right|^{-1}$$

for a fixed value of r=0.95 and θ running from 0 to 2π. Each tall spike represents a close approach to a zero of the divisor series. Here, $\sigma_2(n)$ is an arithmetic series, specifically, the multiplicative series

$$\sigma_a(n) = \sum_{d|n} d^a$$

where the sum extends over the integer divisors of n.

REFERENCES

[1] Tom M. Apostol. *Modular Functions and Dirichlet Series in Number Theory*. Springer, 2nd ed. edition, 1990.

[2] Alexander Bogomolny. Stern brocot trees. http://www.cut-the-knot.org/blue/Stern.shtml, 1996-2006.

[3] Georg Cantor. On the power of perfect sets of points (1884). In Gerald A. Edgar, editor, *Classics on Fractals*, pages 11–23. Addison-Wesley, 1993.

[4] Robert A. Rankin. *Modular Forms and Functions*. Cambridge University Press, 1977.

[5] Linas Vepstas. Symmetries of period-doubling maps. http://www.linas.org/math/chap-takagi.pdf, 2004.

[6] Linas Vepstas. Lattice models and fractal measures. http://www.linas.org/math/lattice.pdf, 2006.
[7] Linas Vepstas. On the minkowski measure. *ArXiv*, arXiv:0810.1265, 2008.